Published in final edited form as:
J Am Soc Nephrol. 2005 October ; 16(10): 2847–2851.

The *kd/kd* Mouse Is a Model of Collapsing Glomerulopathy

Laura Barisoni[*], **Michael P. Madaio**[‡], **Maria Eraso**[†], **David L. Gasser**[§], and **Peter J. Nelson**[†]
[*] *Department of Pathology and*

[†] *Division of Nephrology, New York University School of Medicine, New York, New York; and the*

[‡] *Renal Electrolyte & Hypertension Division, and*

[§] *Department of Genetics, University of Pennsylvania School of Medicine, Philadelphia, Pennsylvania*

Abstract

Collapsing glomerulopathy (CG) is associated with disorders that markedly perturb the phenotype of podocytes. The *kd/kd* mouse has been studied for immune and genetic causes of microcystic tubulointerstitial nephritis with little attention to its glomerular lesion. Because histologic examination revealed classic morphologic features of CG, the question arises whether podocytes in *kd/kd* mice exhibit additional phenotypic criteria for CG. Utilizing Tg26 mice as a positive control, immunohistochemical profiling of the podocyte phenotype was conducted simultaneously on both models. Similar to Tg26 kidneys, podocytes in *kd/kd* kidneys showed *de novo* cyclin D1, Ki-67, and desmin expression with loss of synaptopodin and WT-1 expression. Electron micrographs showed collapsed capillaries, extensive foot process effacement, and dysmorphic mitochondria in podocytes. These results indicate that the *kd/kd* mouse is a model of CG and raise the possibility that human equivalents of the *kd* susceptibility gene may exist in patients with CG.

Since its first clinicopathologic descriptions in the 1980s, collapsing glomerulopathy (CG) is increasingly recognized as the cause of renal failure in humans and experimental animals (1–7). In addition to the unique glomerular morphology of hyperplastic and hypertrophic podocytes overlying collapsed capillary loops (1,2), a consistent feature of CG is the marked perturbation to the mature phenotype of podocytes in diseased glomeruli (8–13). This dysregulated podocyte phenotype is captured by select immunohistochemical markers and segregates the podocyte injury in CG from other podocytopathies (8–13). Indeed, the application of these morphologic and immunohistochemical criteria has been instrumental in characterizing several new murine models with similarities to human CG over the last two years (3–7), each in turn furthering knowledge that disruption of normal podocyte function, whether from intrinsic or extrinsic insults, is a critical step in the development of CG.

The *kd/kd* mouse was first described over three decades ago as a distinctive model of spontaneous proliferative disease of renal epithelium in a subline of CBA/CaH mice (14). Since then, the *kd/kd* mouse has been studied for immune and genetic causes of its prominent microcystic tubulointerstitial nephritis with little attention to the accompanying glomerular lesion (15–19). Recently, the susceptibility gene for renal disease in *kd/kd* mice was mapped and found to encode a prenyltransferase-like mitochondrial protein (PLMP) with shared homology to human transprenyltransferase, human geranylgeranyl pyrophosphate synthase, and a putative human tumor suppressor protein (16,19). C57BL/6 (B6) mice bred homozygous for this mutant allele manifest a tubulointerstitial disease identical to the founder strain with variable onset no earlier than 8 wk of age that ultimately progresses to end-stage renal disease

Address correspondence to: Dr. Peter J. Nelson, Division of Nephrology, New York University School of Medicine, OBV-CD696, 550 First Avenue, New York, NY 10016. Phone: 212-263-7681; Fax: 212-263-7683; E-mail: nelsop02@popmail.med.nyu.edu.

by 16 to 40 wk of age (18,19). Introduction of a wild-type PLMP transgene into B6 *kd/kd* mice can rescue this renal disease (19), suggesting that the *kd* susceptibility gene is required, but perhaps not sufficient alone, for the development of nephropathy in this model. Because histologic examination of glomeruli in diseased B6 *kd/kd* mice revealed glomerular collapse and extensive glomerulosclerosis with hypertrophy and hyperplasia of overlying podocytes (Figure 1), we asked whether the additional immunohistochemical and ultrastructural criteria that define CG exist in B6 *kd/kd* mice. Using heterozygous Tg26 mice as a previously characterized positive control for murine CG (20,21), quantitative profiling of the phenotype of podocytes was conducted simultaneously across the two models.

Materials and Methods

Mice

All studies on Tg26 and B6 *kd/kd* tissues complied with Institutional Animal Care and Use Committee regulations of the New York University School of Medicine and the University of Pennsylvania School of Medicine, respectively. Archival formalin-fixed, paraffin-embedded kidneys from six homozygous B6 *kd/kd* mice ranging in ages from 15 to 43 wk and from two 15-wk-old wild-type B6 controls were studied. Archival formalin-fixed, paraffin-embedded kidneys from three 6-wk-old heterozygous Tg26 mice and from one 6-wk-old nontransgenic littermate were used as positive and negative controls, respectively, for murine CG (20,21).

Histopathology

Three-μm thick serial sections from each specimen were stained with hematoxylin and eosin (H&E), trichrome, periodic-acid schiff (PAS), or silver. Quantitative histopathology for the extent of glomerular sclerosis, capillary tuft collapse with overlying podocyte hypertrophy and hyperplasia, tubular microcysts, acute tubular injury, tubular atrophy, and interstitial inflammation and fibrosis, was singularly evaluated across the entirety of each section. This quantitation was performed as follows: The percent of all glomeruli with sclerosis (defined as segmental or global solidification of the glomerular tuft on silver or trichrome stain); the percent of all glomeruli with collapse (defined as wrinkling and folding of the glomerular basement membranes of any portion of the capillary tuft on silver stain) with overlying podocyte hypertrophy and hyperplasia, scaled as zero (none), +/− (1 to 5%), 1+ (6 to 25%), 2+ (26 to 50%), or 3+ (>51%); the percent area of the total tubuloin-terstitial compartment with tubular microcysts (defined as tubules dilated at least 4 times the normal diameter), acute tubular injury (defined as flattening of the tubular epithelium, loss of the brush border, or blebbing of the cytoplasm and nuclear hyperchromasia with prominent nucleoli), tubular atrophy (defined as thickened tubular basement membranes with small cuboidal tubular cells), or interstitial inflammation and fibrosis, scaled as zero (none), +/− (1 to 5%), 1+ (6 to 25%), 2+ (26 to 50%), or 3+ (>51%).

Immunohistochemistry on 3-μm thick serial sections from each specimen to detect changes to the phenotype of mature podocytes was performed using primary antibodies to mark podocyte cell-cycle engagement (cyclin D1, clone SP4, Lab Vision, Fremont, CA), podocyte cell-cycle progression (Ki-67, clone SP6, Lab Vision), the state of podocyte differentiation (synaptopodin, mouse monoclonal, gift of Dr. Peter Mundel, Mount Sinai School of Medicine, New York, NY; WT-1, clone 6F-H2, NovoCastra, Newcastle, UK), and podocyte injury (desmin, clone D33, DAKO, Carpinteria, CA) as described previously on Tg26 kidneys (20, 21). Sections stained for synaptopodin or desmin were counterstained with hematoxylin, and sections stained with cyclin D1, Ki-67, or WT-1 were counterstained with PAS. Quantitation of the change in podocyte phenotype in each mouse was calculated as the percent of all nonglobally sclerotic glomeruli containing podocytes with cyclin D1 in one or more nuclei, Ki-67 in one or more nuclei, desmin in at least one segmental distribution, loss of WT-1 in at

least one segmental distribution, or with trace or less synaptopodin in the cytoplasm. Globally sclerotic glomeruli were excluded in the analysis due to the absence of podocytes.

Ultrastructural Analysis

Small samples of renal cortex from B6 *kd/kd* mice were fixed in 2.5% glutaraldehyde and 2.0% paraformaldehyde in 0.1 M sodium cacodylate buffer, pH 7.4, overnight at 4°C. Samples were postfixed with 2.0% osmium tetroxide in 0.1 M cacodylate buffer for 1 h at 4°C. After additional washing in 0.1 M cacodylate buffer and distilled H_2O, samples were stained with 2% aqueous uranyl acetate for 30 min at room temperature. Samples were then rinsed in distilled H_2O, dehydrated, infiltrated, and embedded in Embed 812 (Electron Microscopy Science, Fort Washington, PA). Sections were examined in a JEOL100CX electron microscope. Digital images recorded on a Hamamatsu camera were analyzed for the presence of folding and wrinkling of the glomerular basement membrane and foot process effacement.

Results and Discussion

The glomerular lesion of collapsing glomerulopathy is defined morphologically by the presence of hyperplastic and hypertrophic podocytes overlying collapsed capillary loops in either a segmental or global distribution within the glomerular tuft (1,2). These diseased podocytes undergo a marked perturbation in their mature, quiescent phenotype, characterized by proliferation and dedifferentiation, which is not observed in other proteinuric lesions (8–13). Concurrent examination and quantitation of the morphologic injury within glomeruli of B6 *kd/kd* and Tg26 mice, coupled with quantitative profiling of the podocyte phenotype by immunohistochemical markers, demonstrate that the renal disease in B6 *kd/kd* mice fulfills the criteria for CG (Figures 1 and 2;Table 1). Similar to CG in Tg26 mice (20,21), diseased glomeruli in B6 *kd/kd* mice show segmental and global sclerosis and collapse of capillary loops with folding and wrinkling of the glomerular basement membrane, extensive foot process effacement with marked condensation of the actin cytoskeleton and focal loss of primary processes of podocytes, and hyperplastic and hypertrophic podocytes with *de novo* cyclin D1, Ki-67, and desmin expression and reduced synaptopodin and WT-1 expression. In addition to these significant alterations to podocytes, focal injury to the parietal epithelium lining Bowman's capsule is evident in B6 *kd/kd* mice. Despite the variable, age-dependent penetrance of CG in B6 *kd/kd* mice, there appears to be a positive correlation suggesting causality between the extent of glomerular injury and the downstream tubulointerstitial disease in each animal. Together, these data indicate that the B6 *kd/kd* mouse is a previously unrecognized model of CG. Moreover, similar to prior observations of changes to the morphology of mitochondria in the tubular epithelium of B6 *kd/kd* mice (19), abnormal mitochondria are also found in diseased podocytes.

The exact pathogenic steps whereby mutant PLMP causes CG in B6 *kd/kd* mice are not known. Antisera to PLMP localize to dysmorphic mitochondria in renal epithelium of B6 *kd/kd* mice (19). This suggests that mutant PLMP might directly alter mitochondrial function in podocytes, lowering the threshold to injury from energetic stress. This is an attractive hypothesis as CG and focal segmental glomerulosclerosis can develop in patients with genetically-acquired mitochondrial cytopathies (22,23). Furthermore, CG is associated with a growing list of disease stresses (1). If this is indeed correct, B6 *kd/kd* mice would represent the first model of CG due to a mitochondrial disorder, providing a ready system to investigate how environmental factors may influence the manifestation of this abnormality within podocytes. Interestingly, bisphosphonate drugs, small molecules linked to podocyte injury and CG in humans (24,25), can perturb mitochondrial function (26), and human mitochondrial transprenyltransferases sharing homology with PLMP contain specificity determining residues for bisphosphonate binding (*i.e.*, the amino acid sequence DD*XX*D). However, the extent to which bisphosphonates

interact with and inhibit human transprenyltransferases is still unclear (Eric Oldfield, University of Illinois at Urbana-Champaign, personal communication).

Alternatively but not mutually exclusively, an aberrant autoimmune-like response to renal parenchymal damage specific to B6 mice may dictate the development of CG in this model, as suggested by prior studies on B6 *kd/kd* mice (18). Although the phenotypic manifestation of renal disease after transfer of the *kd* susceptibility gene to B6 mice, a strain biased toward T-helper type 1 immunity (27), appears to be identical to that of the founder strain, we do not know if the degenerate glomeruli, glomerulosclerosis, and albuminuria noted in the original report on CBA/CaH *kd/kd* mice (14) is a product of the same podocytopathy reported here (*i.e.*, CBA/CaH *kd/kd* tissues are no longer available). Indeed, although specific genes that may modify the nephropathy in B6 *kd/kd* have not been identified, the CG in B6 *kd/kd* mice may ultimately be attributable to background genetic differences between strains of mice. For example, using a mouse genetics approach with Tg26 mice to investigate the racial predilection of HIV-induced CG, Gharavi *et al.* identified susceptibility loci and strain-specific modifications to specific features of the renal disease in this model (28), including amelioration by BALB/C mice, a strain biased toward T-helper type 2 immunity (27). These intriguing observations regarding what is likely to be a polygenic disease raise the possibility that human equivalents of the *kd* susceptibility gene may exist and predispose some patients to develop CG. Further studies on B6 *kd/kd* mice, the first model of CG caused by a spontaneously occurring mutation identified through forward genetics, not a product of reverse genetics (3, 4,6,7,20), and of patients with CG will help answer these questions.

Acknowledgements

We thank Ali Gharavi and David B. Thomas for critical reading of the manuscript, Ke Lin for excellent technical support, Ray Meade from the Biomedical Imaging Core of the University of Pennsylvania for the electron microscopy, and David B. Thomas, J. Charles Jennette, and Surya Seshan for reviewing the pathology in a blinded fashion. This work was supported by National Institutes of Health grants DK55852 (D.L.G.) and DK065498 (P.J.N.).

References

1. Laurinavicius A, Rennke HG. Collapsing glomerulopathy: A new pattern of renal injury. Semin Diagn Pathol 2002;19:106–115. [PubMed: 12180632]
2. Barisoni L, Kopp JB. Modulation of podocyte phenotype in collapsing glomerulopathies. Microsc Res Tech 2002;57:254–262. [PubMed: 12012394]
3. Eremina V, Sood M, Haigh J, Nagy A, Lajoie G, Ferrara N, Gerber HP, Kikkawa Y, Miner JH, Quaggin SE. Glomerular-specific alterations of VEGF-A expression lead to distinct congenital and acquired renal diseases. J Clin Invest 2003;111:707–716. [PubMed: 12618525]
4. Smeets B, Te Loeke NA, Dijkman HB, Steenbergen ML, Lensen JF, Begieneman MP, van Kuppevelt TH, Wetzels JF, Steenbergen EJ. The parietal epithelial cell: A key player in the pathogenesis of focal segmental glomerulosclerosis in Thy-1.1 transgenic mice. J Am Soc Nephrol 2004;15:928–939. [PubMed: 15034095]
5. Hermann M, Shaw S, Kiss E, Camici G, Buhler N, Chenevard R, Luscher TF, Grone HJ, Ruschitzka F. Selective COX-2 inhibitors and renal injury in salt-sensitive hypertension. Hypertension 2005;45:193–197. [PubMed: 15630049]
6. Powell DR, Desai U, Sparks MJ, Hansen G, Gay J, Schrick J, Shi ZZ, Hicks J, Vogel P. Rapid development of glomerular injury and renal failure in mice lacking p53R2. Pediatr Nephrol 2005;20:432–440. [PubMed: 15723268]
7. Matsusaka T, Xin J, Niwa S, Kobayashi K, Akatsuka A, Hashizume H, Wang QC, Pastan I, Fogo AB, Ichikawa I. Genetic engineering of glomerular sclerosis in the mouse via control of onset and severity of podocyte-specific injury. J Am Soc Nephrol 2005;16:1013–1023. [PubMed: 15758046]
8. Bariety J, Nochy D, Mandet C, Jacquot C, Glotz D, Meyrier A. Podocytes undergo phenotypic changes and express macrophagic-associated markers in idiopathic collapsing glomerulopathy. Kidney Int 1998;53:918–925. [PubMed: 9551398]

9. Shankland SJ, Eitner F, Hudkins KL, Goodpaster T, D'Agati V, Alpers CE. Differential expression of cyclin-dependent kinase inhibitors in human glomerular disease: Role in podocyte proliferation and maturation. Kidney Int 2000;58:674–683. [PubMed: 10916090]
10. Barisoni L, Kriz W, Mundel P, D'Agati V. The dysregulated podocyte phenotype: A novel concept in the pathogenesis of collapsing idiopathic focal segmental glomerulosclerosis and HIV-associated nephropathy. J Am Soc Nephrol 1999;10:51–61. [PubMed: 9890309]
11. Barisoni L, Mokrzycki M, Sablay L, Nagata M, Yamase H, Mundel P. Podocyte cell cycle regulation and proliferation in collapsing glomerulopathies. Kidney Int 2000;58:137–143. [PubMed: 10886558]
12. Nagata M, Horita S, Shu Y, Shibata S, Hattori M, Ito K, Watanabe T. Phenotypic characteristics and cyclin-dependent kinase inhibitors repression in hyperplastic epithelial pathology in idiopathic focal segmental glomerulosclerosis. Lab Invest 2000;80:869–880. [PubMed: 10879738]
13. Yang Y, Gubler MC, Beaufils H. Dysregulation of podocyte phenotype in idiopathic collapsing glomerulopathy and HIV-associated nephropathy. Nephron 2002;91:416–423. [PubMed: 12119471]
14. Lyon MF, Hulse EV. An inherited kidney disease of mice resembling human nephronophthisis. J Med Genet 1971;8:41–48. [PubMed: 5098070]
15. Neilson EG, McCafferty E, Feldman A, Clayman MD, Zakheim B, Korngold R. Spontaneous interstitial nephritis in kdkd mice. I. An experimental model of autoimmune renal disease . J Immunol 1984;133:2560–2565. [PubMed: 6384368]
16. Dell KM, Li YX, Peng M, Neilson EG, Gasser DL. Localization of the mouse kidney disease (kd) gene to a YAC/ BAC contig on chromosome 10. Mamm Genome 2000;11:967–971. [PubMed: 11063251]
17. Sibalic V, Fan X, Wuthrich RP. Characterisation of cellular infiltration and adhesion molecule expression in CBA/ CaH-kdkd mice with tubulointerstitial renal disease. Histochem Cell Biol 1997;108:235–242. [PubMed: 9342617]
18. Hancock WW, Tsai TL, Madaio MP, Gasser DL. Cutting edge: Multiple autoimmune pathways in kd/kd mice. J Immunol 2003;171:2778–2781. [PubMed: 12960297]
19. Peng M, Jarett L, Meade R, Madaio MP, Hancock WW, George AL Jr, Neilson EG, Gasser DL. Mutant prenyltransferase-like mitochondrial protein (PLMP) and mitochondrial abnormalities in kd/kd mice. Kidney Int 2004;66:20–28. [PubMed: 15200409]
20. Barisoni L, Bruggeman LA, Mundel P, D'Agati VD, Klotman PE. HIV-1 induces renal epithelial dedifferentiation in a transgenic model of HIV-associated nephropathy. Kidney Int 2000;58:173–181. [PubMed: 10886562]
21. Petermann A, Hiromura K, Pippin J, Blonski M, Couser WG, Kopp J, Mundel P, Shankland SJ. Differential expression of d-type cyclins in podocytes in vitro and in vivo. Am J Pathol 2004;164:1417–1424. [PubMed: 15039229]
22. Hotta O, Inoue CN, Miyabayashi S, Furuta T, Takeuchi A, Taguma Y. Clinical and pathologic features of focal segmental glomerulosclerosis with mitochondrial tRNAL-eu(UUR) gene mutation. Kidney Int 2001;59:1236–1243. [PubMed: 11260383]
23. Scaglia F, Vogel H, Hawkins EP, Vladutiu GD, Liu LL, Wong LJ. Novel homoplasmic mutation in the mitochondrial tRNATyr gene associated with atypical mitochondrial cytopathy presenting with focal segmental glomerulosclerosis. Am J Med Genet A 2003;123:172–178. [PubMed: 14598342]
24. Markowitz GS, Appel GB, Fine PL, Fenves AZ, Loon NR, Jagannath S, Kuhn JA, Dratch AD, D'Agati VD. Collapsing focal segmental glomerulosclerosis following treatment with high-dose pamidronate. J Am Soc Nephrol 2001;12:1164–1172. [PubMed: 11373339]
25. Barri YM, Munshi NC, Sukumalchantra S, Abulezz SR, Bonsib SM, Wallach J, Walker PD. Podocyte injury associated glomerulopathies induced by pamidronate. Kidney Int 2004;65:634–641. [PubMed: 14717935]
26. Lehenkari PP, Kellinsalmi M, Napankangas JP, Ylitalo KV, Monkkonen J, Rogers MJ, Azhayev A, Vaananen HK, Hassinen IE. Further insight into mechanism of action of clodronate: Inhibition of mitochondrial ADP/ATP translocase by a nonhydrolyzable, adenine-containing metabolite. Mol Pharmacol 2002;61:1255–1262. [PubMed: 11961144]
27. Fowell DJ, Locksley RM. Leishmania major infection of inbred mice: Unmasking genetic determinants of infectious diseases. Bioessays 1999;21:510–518. [PubMed: 10402957]

28. Gharavi AG, Ahmad T, Wong RD, Hooshyar R, Vaughn J, Oller S, Frankel RZ, Bruggeman LA, D'Agati VD, Klotman PE, Lifton RP. Mapping a locus for susceptibility to HIV-1-associated nephropathy to mouse chromosome 3. Proc Natl Acad Sci U S A 2004;101:2488–2493. [PubMed: 14983036]

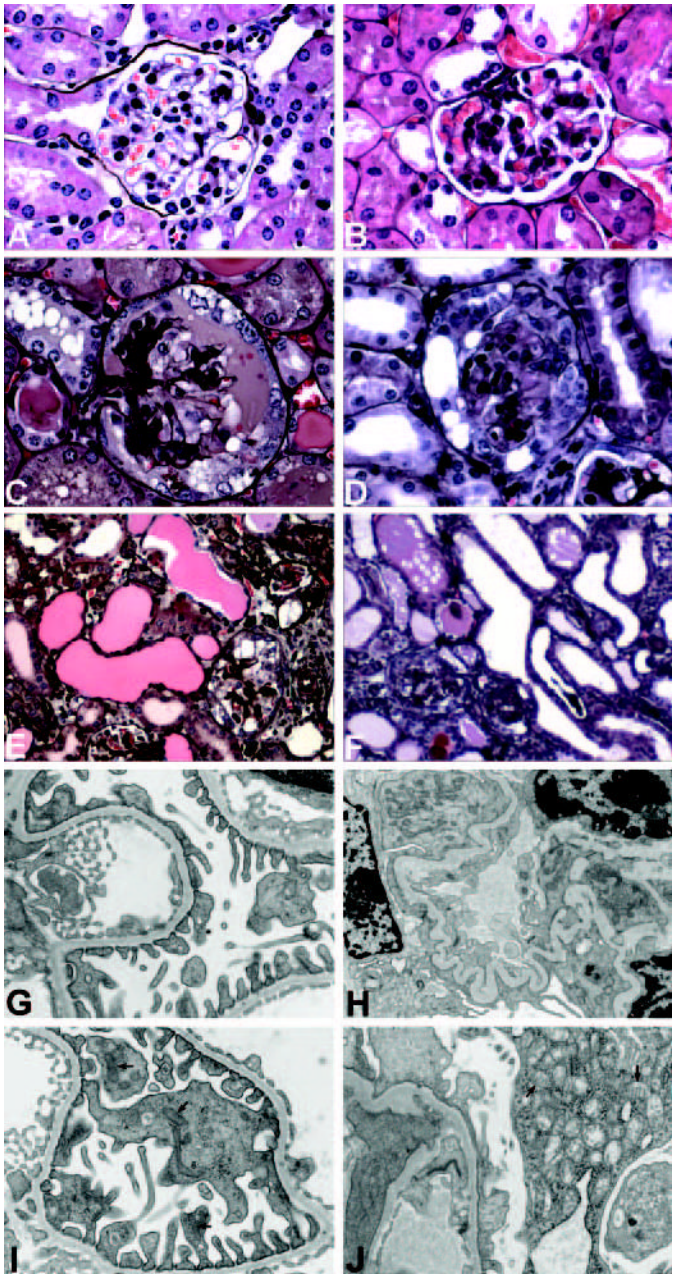

Figure 1.

Collapsing glomerulopathy in B6 *kd/kd* mice. (A) Normal glomerulus in a B6 wild-type mouse. (B) Normal glomerulus in a nontransgenic Tg26 mouse. (C) B6 *kd/kd* mouse with glomerular collapse and podocyte hypertrophy and hyperplasia; focal injury to the parietal epithelium is also noted. (D) Tg26 heterozygote with glomerular collapsing features and prominent podocyte hypertrophy and hyperplasia with pseudocrescent formation and bridging to parietal epithelial cells. (E) B6 *kd/kd* mouse showing glomerular collapse and pseudocrescent formation adjacent to severe tubulointerstitial damage with prominent, protein-filled microcysts. (F) Tg26 heterozygote showing glomerular collapse with pseudocrescent formation adjacent to severe tubulointerstitial damage with prominent microcysts. (G) Electron micrograph of a glomerular capillary in a B6 wild-type mouse shows glomerular basement membranes (GBM) that are normal in thickness and contour, as well as podocytes with well-preserved foot processes. (H)

Electron micrograph of a glomerular capillary in a diseased B6 *kd/kd* mouse shows GBM that are wrinkled and folded (indicating collapse) with subocclusion of the capillary lumen. There is also extensive foot process effacement accompanied by condensation of the actin-based cytoskeleton and swelling of primary processes. (I) A healthy podocyte from a B6 wild-type mouse containing few normal mitochondria with regular matrix density (arrows). (J) A diseased podocyte from a B6 *kd/kd* mouse containing numerous abnormal mitochondria with compressed cristae forming truncated cisternae and granular-appearing matrix (arrows). Magnification, × 400 in A through D, × 100 in E and F, ×25,000 in G through J. The sections in A through F are silver-stained.

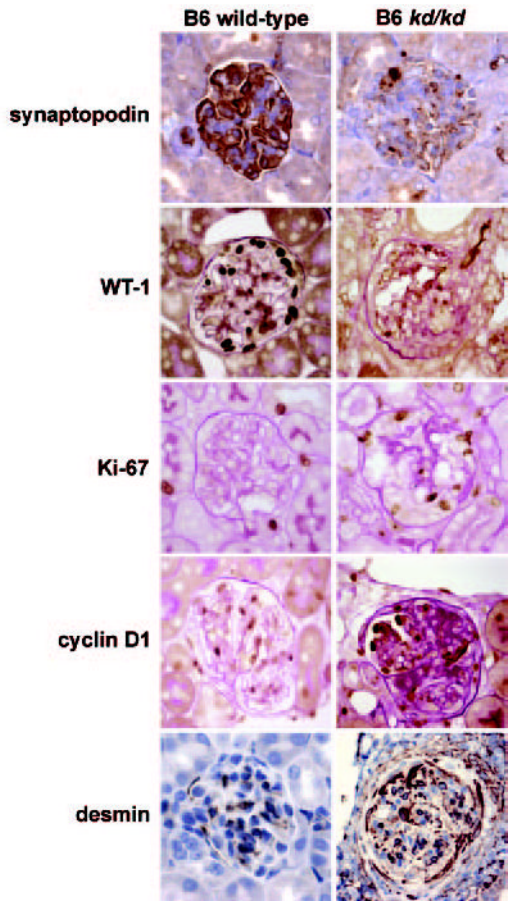

Figure 2.

Comparison of the podocyte phenotype between B6 wild-type and B6 *kd/kd* mice. Synaptopodin stains strongly in the cytoplasm of podocytes in B6 wild-type mice indicating the normal, differentiated state, whereas there is a marked loss of synaptopodin expression in diseased podocytes in B6 *kd/kd* mice. An identical change is observed in the nuclear staining of WT-1, a second marker of podocyte differentiation. Nuclear staining of Ki-67, a marker of cell-cycle progression, is not detected in glomeruli of B6 wild-type mice, but is focally positive in glomerular epithelial cells forming pseudocrescents in B6 *kd/kd* mice. Likewise, nuclear staining of cyclin D1, a marker of cell-cycle engagement, is diffusely negative in podocytes of B6 wild-type mice (but positive in some intracapillary cells), whereas it is detected in podocytes in B6 *kd/kd* mice in areas of podocyte hypertrophy and hyperplasia. Glomerular staining of desmin is found only in mesangial cells in B6 wild-type mice, but is markedly upregulated in injured podocytes in B6 *kd/kd* mice. Magnification, × 400.

Table 1

psing glomerulopathy in B6 *kd/kd* and Tg26 mice: Morphologic injury and changes to the podocyte phenotype

Mouse	Age (wk)	Segmental Collapse (%)	Global Collapse (%)	Segmental Sclerosis (%)	Global Sclerosis (%)	Podocyte Hyperplasia/ Hypertrophy	Microcysts/ Acute Tubular Injury	Interstitial Inflamation	Interstitial Fibrosis and Tubular Atrophy	Synaptopodin (% negative)	WT1 (% negative)	Ki-67 (% positive)	Cyclin D1 (% positive)	Desmin (% positive)
6 wild-type	15	0	0	0	0	0	0	0	0	0	0	0	0	0
6 wild-type	15	0	0	0	0	0	0	0	0	0	0	0	0	0
6 kd/kd	15	0	0	1	1.5	1+	0	0	0	0	0	2.8	0	1.4
6 kd/kd	16	0	0	0	1	+/−	+/−	+/−	+/−	0	6.6	1.5	30.1	0
6 kd/kd	18	4.3	6.1	4.3	6.1	+/−	1+	+/−	+/−	98	71.9	17.6	15.7	7.8
6 kd/kd	21	13.2	25	8.9	11.4	2+	3+	3+	3+	100	33.3	5.5	43.7	16.7
6 kd/kd	22	6.8	0	12.3	0	1+	3+	3+	2+	86	9.4	12.5	57.5	11.3
6 kd/kd	43	8.7	3.5	23.5	55.6	+/−	3+	3+	2+	100	100	5.9	60.7	52.9
g26 ontransgenic	6	0	0	0	0	0	0	0	0	0	0	0	0	0
g26 eterozygote	6	2.6	0	25.7	0	2+	3+	1+	+/−	17.2	100	93.1	86.2	69.2
g26 eterozygote	6	3.8	0	47.2	13.2	2+	3+	1+	+/−	54.3	67.4	54.3	82.6	100
g26 eterozygote	6	1.2	0	58.3	41.7	3+	3+	1+	1+	94	54.8	78.6	69.3	100